

ρ/ω properties from dilepton spectra in pA reactions at 12 GeV *

E. L. Bratkovskaya

Institut für Theoretische Physik, Universität Giessen
35392 Giessen, Germany

Abstract

The dilepton production from pC and pCu collisions at $T_{lab} = 12$ GeV is calculated using the semi-classical BUU transport model, that includes the off-shell propagation of vector mesons nonperturbatively and calculates the width of the vector mesons dynamically. It is found that the collisional broadening of the vector meson width and dropping vector meson masses lead to a small enhancement of the dilepton yield below the ω meson mass pole in pCu collisions compared to pC , which is, however, not sufficient to explain the enhanced production of dileptons as observed in the experiment by the KEK-PS E325 collaboration. It is argued that such in-medium effects are expected to be small due to kinematical reasons – the dominant part of vector mesons shine dileptons and decay outside the nucleus due to the finite formation time for ρ and ω mesons, which is large by Lorentz covariance since the produced vector mesons move with high velocity relative to the target nucleus.

PACS: 25.75.Dw, 13.30.Ce, 12.40.Yx, 12.40.Vv, 25.40.-h

Keywords: particle and resonance production; leptonic and semileptonic decays; hadron models; vector-meson dominance; nucleon-induced reactions

The modification of hadron properties in nuclear matter is of fundamental interest. Dilepton data from heavy-ion experiments at SPS energies [1, 2] have provided first experimental evidence for a change of the vector meson properties in the nuclear medium, however, the heavy-ion data can be interpreted within different scenarios of in-medium modifications, i.e. by the dropping mass scenario or the collisional broadening approach (cf. the reviews [3, 4, 5] and Refs. therein).

Since in heavy-ion experiments the nuclear matter is probed at different densities and temperatures within the complex dynamical evolution, it is very useful to have independent experimental information from photon-nucleus, pion-nucleus or proton-nucleus reactions, where the properties of vector mesons are probed at normal nuclear density or below.

Such information has been provided recently by the KEK-PS E325 collaboration, that has measured the dilepton spectrum in the mid-rapidity region from pC and pCu collisions

*Supported by Forschungszentrum Jülich

at 12 GeV [6]. A significant difference in the mass spectra below the ω meson mass pole has been observed between pC and pCu reactions. This difference has been interpreted as a modification of the vector meson properties in nuclear matter [6].

In this work the question of in-medium modifications of the ρ, ω meson properties is studied within the semi-classical BUU transport approach of Refs. [7, 8]. This model is based on the resonance concept of nucleon-nucleon and meson-nucleon interactions at low invariant energy \sqrt{s} [9] by adopting all resonance parameters from the Manley analysis [10]. The high energy collisions (multiparticle production) – above $\sqrt{s} = 2.6$ GeV for baryon-baryon collisions and $\sqrt{s} = 2.2$ GeV for meson-baryon collisions – are described by the LUND string fragmentation model FRITIOF [11] with a formation time $\tau_F = 0.8$ fm/c. This aspect is similar to that used in the HSD (Hadron-String-Dynamics) approach [4, 12] and the UrQMD model [13]. This combined resonance-string approach allows to calculate particle production in baryon-baryon and meson-baryon collisions from low to high energies. The collisional dynamics for proton-nucleus reactions, furthermore, is described by the coupled-channel BUU transport approach [7, 8] that is based on the same elementary cross sections. Furthermore, the model has been extended to include the off-shell propagation of vector mesons nonperturbatively [14] and to calculate the width of the vector mesons dynamically, which is consistent with the vector meson production/absorption amplitudes (or probabilities) [7].

The dilepton production within the resonance-string model is treated (as described in Ref. [14]) via the production of resonances R (baryonic or mesonic) in baryon-baryon, meson-baryon or meson-meson collisions, which can couple to dileptons directly or via a further decay into mesons or baryons. The electromagnetic part of all conventional dilepton sources – π^0, η, ω and Δ Dalitz decays, direct decay of vector mesons ρ, ω – are treated in the same way as described in detail in Ref. [15], where dilepton production in elementary pp and pd reactions has been studied.

The treatment of the off-shell propagation of vector mesons is described in Ref. [14] (in line with Refs. [16]), where this model has been applied to study the in-medium modification of vector meson properties in dilepton production in pA collisions at SIS (1–4 GeV) energies. The effects of a collisional broadening of the vector meson width (in line with Refs. [17]) and dropping vector meson masses (according to the Hatsuda and Lee [18] or Brown/Rho scaling [19]) have been investigated in Ref. [14], too. It has been found that the collisional broadening + ‘dropping mass’ scenario leads to an enhancement of the dilepton yield in the invariant mass range $0.5 \leq M \leq 0.75$ GeV, which is most pronounced for heavy systems (up to a factor 2 for $p + Pb$ at 3–4 GeV).

In this work the same transport model – including collisional broadening of the vector meson width plus ‘dropping mass’ scenario – is applied for dilepton production in pC and pCu reactions at $T_{lab} = 12$ GeV as measured by the KEK-PS E325 collaboration [6].

Before showing the results for pA reactions it is worth to present the ‘input’ of the calculations, i.e. the calculated dilepton invariant mass spectra $d\sigma/dM$ for $p + p$ collisions at 12 GeV (Fig. 1). Note, that in Fig. 1 (as well as in all further figures) a mass resolution of $\Delta M = 9.6$ MeV has been included that corresponds to the resolution of Ref. [6] for the ω peak region. The thin lines indicate the individual contributions from the different production channels; i.e. starting from low M : Dalitz decay $\pi^0 \rightarrow \gamma e^+ e^-$ (dot-dot-dashed line), $\eta \rightarrow \gamma e^+ e^-$ (dotted line), $\Delta \rightarrow N e^+ e^-$ (dashed line), $\omega \rightarrow \pi^0 e^+ e^-$ (dot-dashed line), for $M \approx 0.7$ GeV: $\omega \rightarrow e^+ e^-$ (dot-dashed line), $\rho^0 \rightarrow e^+ e^-$ (short dashed line). The full solid line represents the sum of all sources considered here. As seen from Fig. 1, the ρ and

ω decay channels give the dominant contributions at invariant masses $0.6 \leq M \leq 0.75$ GeV, where an excess of the dilepton yield in pCu relative to pC reactions was observed [6].

In Fig. 2 the calculated dilepton invariant mass spectra $d\sigma/dM$ are displayed for $p+C$ (upper part) and $p+Cu$ collisions (lower part) at 12 GeV (including a mass resolution of 9.6 MeV) without in-medium modifications (bare masses; left part), and applying the collisional broadening + dropping mass scenario (right part). The assignment of the individual lines is the same as in Fig.1. Comparing left and right panels one can see that the modification of the dilepton spectrum by including collisional broadening and dropping vector meson masses is rather moderate for the light C -target (upper part of Fig. 2). For the heavy Cu target (lower part of Fig. 2) the shift of the ρ yield to lower invariant masses as well as the secondary ω peak (at $\simeq 0.65$ GeV) is seen due to the dropping of vector meson masses. However, the total enhancement of the dilepton yield is quite small, i.e. less than a factor of 1.5 for $0.6 \leq M \leq 0.75$ GeV.

The direct comparison of the model calculations to the experimental data requires a precise knowledge of the experimental acceptance since in the KEK-PS E325 experiment the low part of the dilepton spectra was significantly suppressed by the geometry of the detectors and nontrivial electronic cuts. Furthermore, the combinatorial background – from a mixing of $e^-\pi^+$ and $e^+\pi^-$ pairs – was not subtracted from the data [6]. Since the full experimental acceptance is not available, a normalization procedure (described below) has been applied to compare the calculated spectra to the experimental data [6].

The experimental data – solid histogram in Fig. 3 – have been fitted in Ref. [6] by the sum of the amplitudes of $\rho/\omega \rightarrow e^+e^-$, $\phi \rightarrow e^+e^-$, $\eta \rightarrow e^+e^-$ and the combinatorial background (dotted lines in Fig. 3, denoted as 'bg') using a four parameter fit. The mass shape of the ρ , ω and ϕ mesons has been taken of the Breit-Wigner form with the natural widths 150, 8.41 and 4.43 MeV (cf. Fig. 3 from Ref. [6]). The normalization of the transport calculations is done in a such way that the integral over the $\omega \rightarrow e^+e^-$ contribution for the bare mass cases (i.e. without in-medium effects) is the same as for the experimentally fitted ω contribution. The same normalization factor is used for the calculations with collisional broadening + dropping masses. Also the combinatorial background (taken from Ref. [6]) is added to the calculated spectra.

It is worth to point out, that an application of the acceptance cuts as described in Ref. [6], i.e. the rapidity cut $0.6 \leq y \leq 2.2$, the transverse momentum cut $p_T \leq 1.5$ GeV, the cut in the opening angle of the e^+e^- pairs $50^\circ \leq \Theta_{open} \leq 150^\circ$, and the restriction that the electron and positron are detected in different detector arms (cf. Fig. 1 in Ref. [6]), leads to a suppression of the dilepton yield by about of a factor of 9 for $M \geq 0.5$ GeV and does not change the shape of the spectra. At low M these cuts suppress the dilepton spectra more effective, however, further 'electronic' acceptance cuts must be applied to reproduce exactly the shape of the measured spectra. Due to this reason only the M -interval $0.45 \leq M \leq 0.9$ GeV is considered, where an excess of the dilepton yield has been observed.

The comparison of the calculated results with the experimental data (histograms) is shown in Fig. 3 for $p+C$ (upper part) and $p+Cu$ collisions (lower part). The solid lines indicate the calculations without in-medium modifications (bare masses), the dot-dashed lines correspond to a calculation including the collisional broadening + dropping mass scenario. The individual contributions are indicated as ' ρ ', ' ω '; the lines marked as 'sum+bg' show the sum of the dilepton contributions and the combinatorial background

(dotted lines 'bg') as taken from Ref. [6].

Note, that the ρ -contribution in Fig. 3 (as well as in Figs. 1,2) is asymmetric in mass due to the fact that the dilepton decay leads to a multiplication of the ρ -spectral function by $1/M^3$ (cf. Ref. [15]). This is in contrast to the assumption made in Ref. [6]; the same holds for the ω mesons. However, accounting for the $1/M^3$ factor for the ω and ρ dilepton yields changes the experimentally fitted curves by a few percent only, which does not influence the normalization used here (as well as the conclusions of Ref. [6]).

One can see from Fig. 3 that the pC data are roughly reproduced by the calculations within the statistics achieved experimentally, whereas the pCu data are underestimated for $0.55 \leq M \leq 0.75$ GeV. Thus, the excess of the dilepton yield in pCu relative to pC reactions can not be explained neither by the bare mass calculations nor by including in-medium effects such as collisional broadening and dropping vector masses, which gives only a tiny enhancement of the dilepton yield (as mentioned above) by less than a factor of 1.5.

Note, that the calculated yield is higher than the results of the fit procedure from Ref. [6] for $0.55 \leq M \leq 0.75$ GeV. That is due to the fact that the calculated ρ contribution is slightly higher than the fitted one (corrected by the factor $1/M^3$). In the simulations of Ref. [6] the assumption was made, that all vector mesons are produced from primary nucleon-nucleon collisions at 12 GeV with equal ρ and ω production cross sections (in line with the experimental data on ρ , ω production at 12 GeV/c from Ref. [20]). This leads to an about equal dilepton yield from ρ and ω mesons, especially using the assumption about the instantaneous decay of vector mesons into dileptons, i.e. without performing the time integration of the shining dileptons during the life time of the mesons (before their nonleptonic decays such as $\rho^0 \rightarrow \pi^+\pi^-$, $\omega \rightarrow \pi^+\pi^-\pi^0$). Note, that the time integration procedure, as described in Ref. [21], is important for a correct evaluation of the dilepton spectra due to the absorption of vector mesons in the nucleus.

In the resonance-string model the vector mesons are dominantly produced in first nucleon-nucleon collisions via baryon-baryon (BB) string excitations and decays with production cross sections as in Ref. [20]. However, ρ, ω mesons can be also produced by secondary meson-baryon (mB) collisions and the ρ mesons additionally by the decay of baryonic resonances (e.g. $D_{13}(1520)$) formed in primary BB or secondary mB collisions. The mB and resonance production mechanisms are especially important for heavy nuclei and give an additional yield of ρ mesons. In numbers: in pC collisions $\sim 90\%$ of ρ and $\sim 95\%$ of ω mesons are produced by BB string decays, $\sim 3\%$ of ρ and $\sim 5\%$ of ω by the mB string formation or by secondary mB collisions and $\sim 7\%$ of ρ by the decays of $D_{13}(1520)$ and other baryonic resonances coupled to the ρ . For the heavy Cu target $\sim 70\%$ of ρ and $\sim 85\%$ of ω mesons are produced by BB string decays, $\sim 10\%$ of ρ and $\sim 15\%$ of ω by mB interaction and $\sim 15\%$ of ρ by the decays of $D_{13}(1520)$ and other baryonic resonances. Note, that the fraction of ω mesons produced by mB interactions is slightly larger than of ρ 's due to the fact that in low energy secondary mB collisions baryonic resonances – that couple to the ρ – are excited predominantly.

The ρ mesons live for a very short time and shine dileptons with high intensity (as compared to the ω mesons) before decaying into two pions or being absorbed in the nuclear interior. The ω mesons are longer living particles and they can be absorbed by nucleons in the nucleus, too, before their natural 'death', i.e. 3 pion decay. The ω absorption violates the $A^{2/3}$ scaling (where A is the target mass number), i.e. the scaling of the dilepton rate from pA reactions is expected to be higher by a factor of $A^{2/3}$ than in $p + p$ collisions [6].

As seen from Fig. 1 and Fig. 2 in the calculations the $A^{2/3}$ scaling is practically fulfilled for the light C target, however, for the heavy Cu target the ω yield is about $\sim 30\%$ lower as expected from $A^{2/3}$ scaling due to ω absorption.

For a better understanding, why the in-medium effects are so small, the average density distribution of a Cu -nucleus at rest in the laboratory is shown in Fig. 4 (upper left part) as well as the spatial distribution in the first pN collisions (upper right part). Here the spatial distribution $\frac{1}{b} \frac{dN}{dbdz}$ is displayed in cylindrical coordinates $b = (x^2 + y^2)^{1/2}$ and z , where z is directed along the beam axis and the proton is impinging on the nucleus from the left side. The lower part of Fig. 4 displays the spatial distribution for ρ -meson (left part) and ω -meson (right part) decays to dileptons for the bare masses case. As mentioned above, at 12 GeV bombarding energy most of the ω and ρ mesons – formed in primary pN collisions – move with a high velocity through the target. Contrary to low energy collisions (cf. Fig. 1 from Ref. [14]), most of the ρ 's and ω 's are shining dileptons and decaying outside the nucleus; this holds especially for ω mesons which have a longer life time such that the ω spatial distribution is more elongated in beam direction than the ρ . In numbers: for the C target only $\sim 2.5\%$ of ω and $\sim 14\%$ of ρ mesons shine dileptons inside the nucleus; for the Cu target $\sim 7\%$ of ω and $\sim 32\%$ of ρ mesons shine e^+e^- pairs inside. For the collisional broadening + dropping mass scenario the fraction of the ρ mesons shining lepton pairs inside increases to $\sim 45\%$ for Cu target due to an enhanced production of ρ mesons with low masses. Thus the dropping mass and collisional broadening effects – which are proportional to the baryon density – do not influence the dilepton spectra very much.

To illustrate the dynamics of pA reactions at 12 GeV, the laboratory rapidity distribution $d\sigma/dy$ is presented in Fig. 5 (upper part) for $\rho \rightarrow e^+e^-$ (dashed lines) and $\omega \rightarrow e^+e^-$ (solid lines) for $p+C$ (left) and $p+Cu$ (right) at 12 GeV. The arrows indicate the experimental rapidity window ($0.6 \leq y \leq 2.2$). The lower part of Fig. 5 shows the momentum distribution $d\sigma/dp$ for $\rho \rightarrow e^+e^-$ (dashed lines) and $\omega \rightarrow e^+e^-$ (solid lines) for $p+C$ (left part) and $p+Cu$ (right part) at 12 GeV calculated with the experimental cuts on rapidity ($0.6 \leq y \leq 2.2$) and $p_T < 1.5$ GeV/c.

One can see from the upper part of Fig. 5 that the rapidity distribution for $\rho \rightarrow e^+e^-$ and $\omega \rightarrow e^+e^-$ are similar for pC collisions; only the ρ distribution is shifted slightly to the low rapidity region due to the fact that the ρ spectral function is broad and ρ mesons can be produced with low masses, too. This shift is more pronounced for the heavy Cu target, where more ρ mesons are formed with lower masses via baryonic resonance decays. Also, the ω absorption effect, as discussed above, is well seen.

The experimental acceptance selects dilepton events at mid-rapidity with momentum distributions shown in the lower part of Fig. 5. It is seen, that the ρ 's and ω 's are very fast; the corresponding Lorentz γ -factors (in the laboratory frame) are in the range $1 < \gamma < 6.5$. One has to recall that the vector mesons produced by strings can shine dileptons only after they are formed as physical particles (not as pre-resonant or quark states). The formation time τ_F , which denotes the time between the formation and fragmentation of the string in the individual hadron-hadron center-of-mass system is taken to be $\tau_F = 0.8$ fm/c (cf. [4, 12, 13]). Due to covariance the hadrons with finite momentum p then are formed at the actual time $\Delta t = \gamma\tau_F$ (in the laboratory frame). During this time Δt the pre-formed particles (strings) are moving with high velocities and start to shine dileptons only either outside the nucleus or closer to the nuclear surface (cf. Fig. 4). This kinematical effect suppresses in-medium effects. It is worth to point out, that for low energy pA collisions

the in-medium effects are expected to be larger since the vector mesons are formed (and shine dileptons) more abundantly inside the nucleus [14].

One might argue that the formation time τ_F could be substantially smaller than the value of 0.8 fm/c adopted here (or values of 1-2 fm/c depending on the hadron-species as used in UrQMD [13]). In fact, when assuming $\tau_F = 0$, the amount of in-medium ρ decays for $p + Cu$ increases to $\sim 50\%$ (and to $\sim 65\%$ for the collisional broadening + dropping mass scenario) and to $\sim 12\%$ for the ω mesons, respectively. In this limit the calculated dilepton yield indeed becomes comparable to the experimental spectrum for $p + Cu$. Furthermore, the transport calculation for $\tau_F = 0$ roughly correspond to the Glauber limit for vector meson production and absorption in $p + A$ reactions. However, as shown in the context of heavy-ion collisions [12], a reduction of τ_F leads to an unphysical production multiplicity of mesons (as well as to rapidity and momentum distributions of baryons and mesons that are incompatible with the experimental data) since the rescattering rate becomes too high (some examples for $p + A$ reactions are also shown in Ref. [8]). Furthermore, experimental studies on \bar{p} production and reabsorption at 12.3 and 17.5 GeV/c in $p + A$ reactions by the E910 collaboration [22] have shown that the formation time of antiprotons might be even larger than 0.8 fm/c in order to describe the low amount of \bar{p} reabsorption in $p + A$ reactions.

In summary: the dilepton production from pC and pCu collisions at $T_{lab} = 12$ GeV has been calculated using a combined resonance-string transport approach. It has been found that the enhanced production of dileptons below the ω meson mass pole in pCu collisions compared to pC – as observed in the experiment by the KEK-PS E325 collaboration – cannot be explained by collisional broadening nor dropping vector meson masses. It has been argued that such in-mediums effects are expected to be small due to kinematical reasons, i.e. the dominant part of vector mesons shine dileptons and decay outside the nucleus due to a finite hadron formation time $\Delta t = \gamma\tau_F$.

Furthermore, the dropping mass scenario should be questionable especially for ρ mesons within the momentum range shown in Fig. 5 since dispersion relations – as employed by Eletsky and Ioffe [23] and Kondratyuk et al. [24] – lead to repulsive ρ meson potentials for such high momenta. To clarify such experimental and/or theoretical inconsistencies high accuracy dilepton spectra within different momentum bins are urgently needed.

The author is grateful to U. Mosel for pointing out this problem, to K. Ozawa for the explanations of the KEK-PS E325 experiment, and to W. Cassing for valuable discussions and a critical reading of the manuscript.

References

- [1] G. Agakichiev et al., Phys. Rev. Lett. 75 (1995) 1272; Th. Ullrich et al., Nucl. Phys. A 610 (1996) 317c; A. Drees, Nucl. Phys. A 610 (1996) 536c.
- [2] M. A. Mazzoni, Nucl. Phys. A 566 (1994) 95c; M. Masera, Nucl. Phys. A 590 (1995) 93c; T. Åkesson et al., Z. Phys. C 68 (1995) 47.
- [3] G.E. Brown, M. Rho, nucl-th/0103102, Phys. Rep., in press
- [4] W. Cassing, E. L. Bratkovskaya, Phys. Rep. 308 (1999) 65.

- [5] R. Rapp, J. Wambach, Adv. Nucl. Phys. 25 (2000) 1.
- [6] K. Ozawa et al., Phys. Rev. Lett. 86 (2001) 5019.
- [7] M. Effenberger, E. Bratkovskaya and U. Mosel, Phys. Rev. C 60 (1999) 044614.
- [8] M. Effenberger, Ph.D. Thesis, Univ. of Giessen, 1999; <http://theorie.physik.uni-giessen.de/ftp.html>.
- [9] S. Teis, W. Cassing, M. Effenberger, A. Hombach, U. Mosel, and Gy. Wolf, Z. Phys. A 356 (1997) 421; Z. Phys. A 359 (1997) 297.
- [10] D. M. Manley and E. M. Saleski, Phys. Rev. D 45 (1992) 4002.
- [11] B. Anderson, G. Gustafson and Hong Pi, Z. Phys. C 57 (1993) 485.
- [12] W. Ehehalt and W. Cassing, Nucl. Phys. A 602 (1996) 449.
- [13] S. A. Bass et al., Prog. Part. Nucl. Phys. 42 (1998) 279; J. Phys. G 25 (1999) 1859.
- [14] E.L. Bratkovskaya, Nucl. Phys. A 696 (2001) 309.
- [15] E.L. Bratkovskaya, W. Cassing and U. Mosel, Nucl. Phys. A 686 (2001) 476.
- [16] W. Cassing and S. Juchem, Nucl. Phys. A 665 (2000) 377; A 672 (2000) 417.
- [17] W. Cassing, Ye. S. Golubeva, A. S. Iljinov, and L. A. Kondratyuk, Phys. Lett. 396 B (1997) 26; Ye. S. Golubeva, L. A. Kondratyuk and W. Cassing, Nucl. Phys. A 625 (1997) 832.
- [18] T. Hatsuda and S. Lee, Phys. Rev. C 46 (1992) R34.
- [19] G.E. Brown and M. Rho, Phys. Rev. Lett. 66 (1991) 2720.
- [20] V. Blobel et al., Phys. Lett. 48 B (1974) 73.
- [21] G.Q. Li, C.M. Ko, and G.E. Brown, Nucl. Phys. A 611 (1996) 539.
- [22] I. Chemakin et al., nucl-ex/0107013.
- [23] V.L. Eletsky and B.L. Ioffe, Phys. Rev. Lett. 78 (1997) 1010.
- [24] L. A. Kondratyuk, A. Sibirtsev, W. Cassing, Ye. S. Golubeva, and M. Effenberger, Phys. Rev. C 58 (1998) 1078.

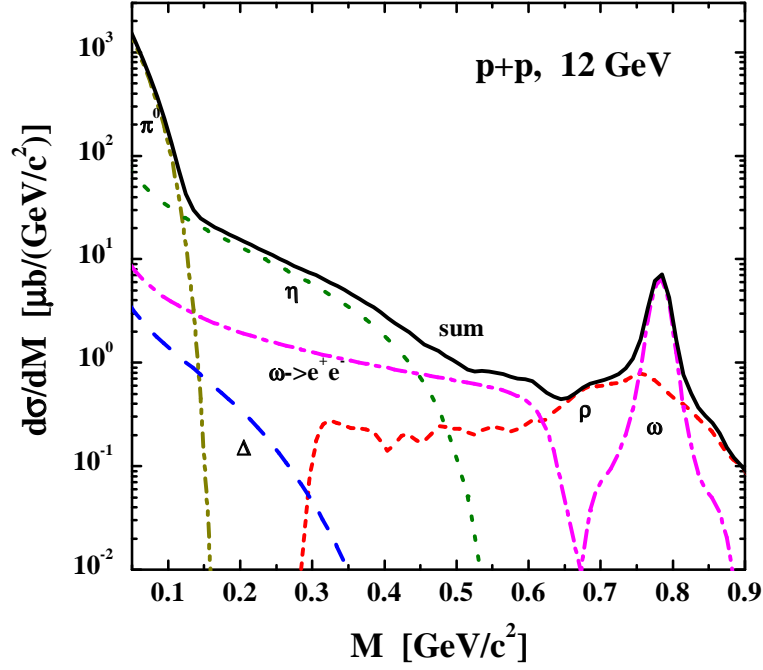


Figure 1: The calculated dilepton invariant mass spectra $d\sigma/dM$ for $p + p$ collisions at 12 GeV (including a mass resolution of 9.6 MeV). The thin lines indicate the individual contributions from the different production channels; *i.e.* starting from low M : Dalitz decay $\pi^0 \rightarrow \gamma e^+ e^-$ (dot-dot-dashed line), $\eta \rightarrow \gamma e^+ e^-$ (dotted line), $\Delta \rightarrow N e^+ e^-$ (dashed line), $\omega \rightarrow \pi^0 e^+ e^-$ (dot-dashed line), for $M \approx 0.7$ GeV: $\omega \rightarrow e^+ e^-$ (dot-dashed line), $\rho^0 \rightarrow e^+ e^-$ (short dashed line). The full solid line represents the sum of all sources considered here.

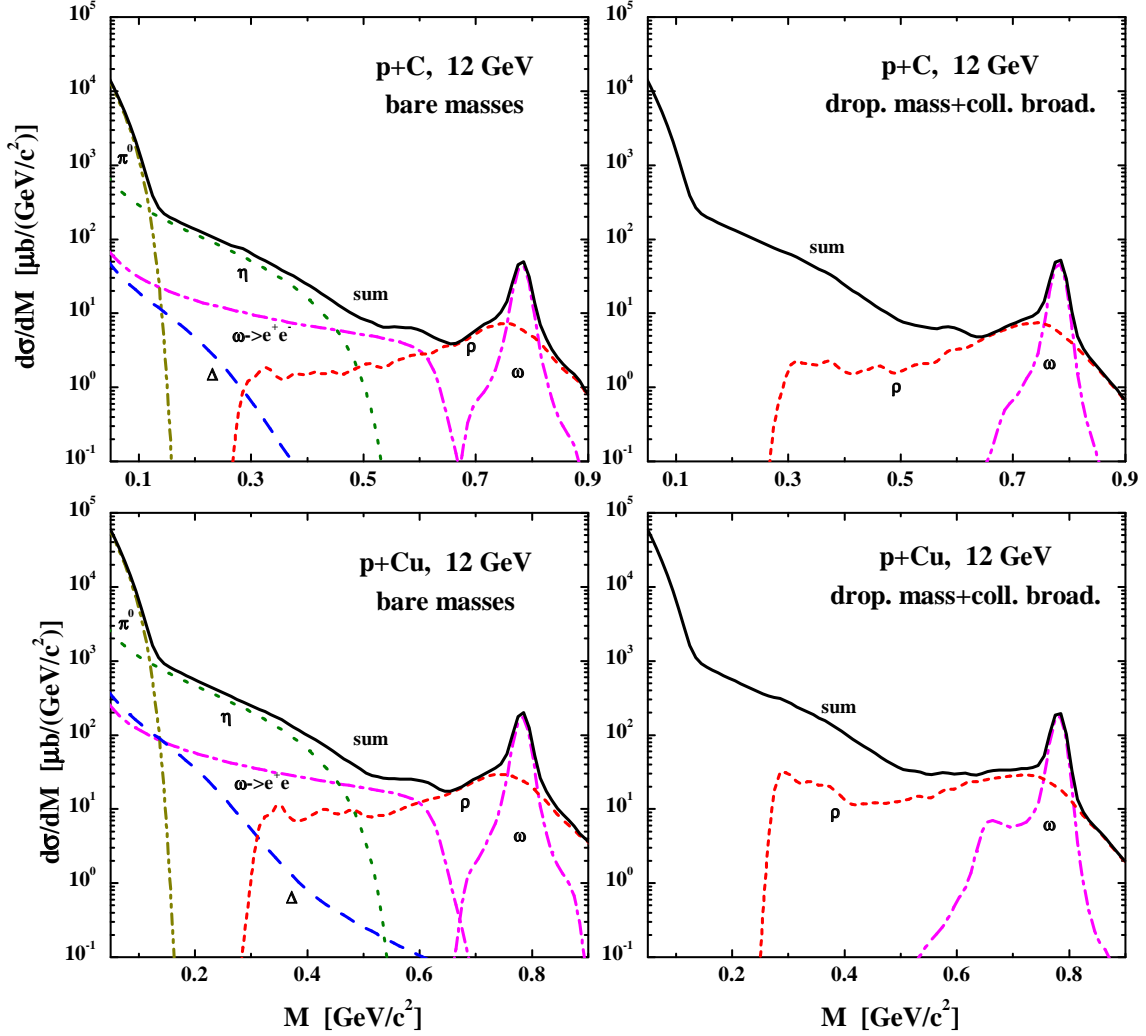


Figure 2: The calculated dilepton invariant mass spectra $d\sigma/dM$ for $p+C$ (upper part) and $p+Cu$ collisions (lower part) at 12 GeV (including a mass resolution of 9.6 MeV) without in-medium modifications (bare masses; left part), and applying the collisional broadening + dropping mass scenario (right part). The assignment of the individual lines is the same as in Fig. 1.

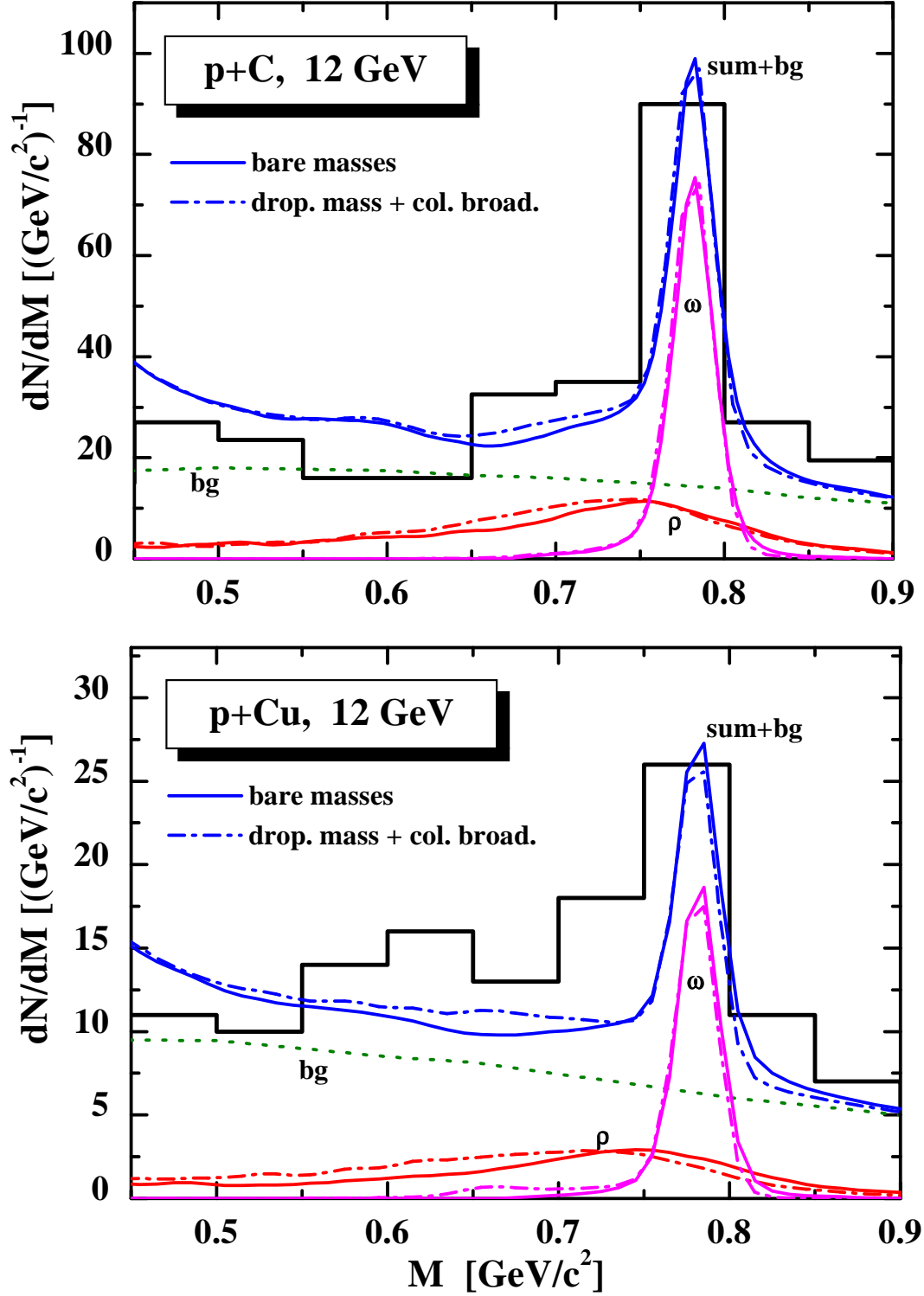


Figure 3: The calculated dilepton invariant mass spectra dN/dM for $p+C$ (upper part) and $p+Cu$ collisions (lower part) at 12 GeV (including an experimental mass resolution of 9.6 MeV) without in-medium modifications (bare masses, solid lines), and applying the collisional broadening + dropping mass scenario (dot-dashed lines) in comparison to the experimental data [6] (histograms). The dotted lines show the combinatorial background from Ref. [6].

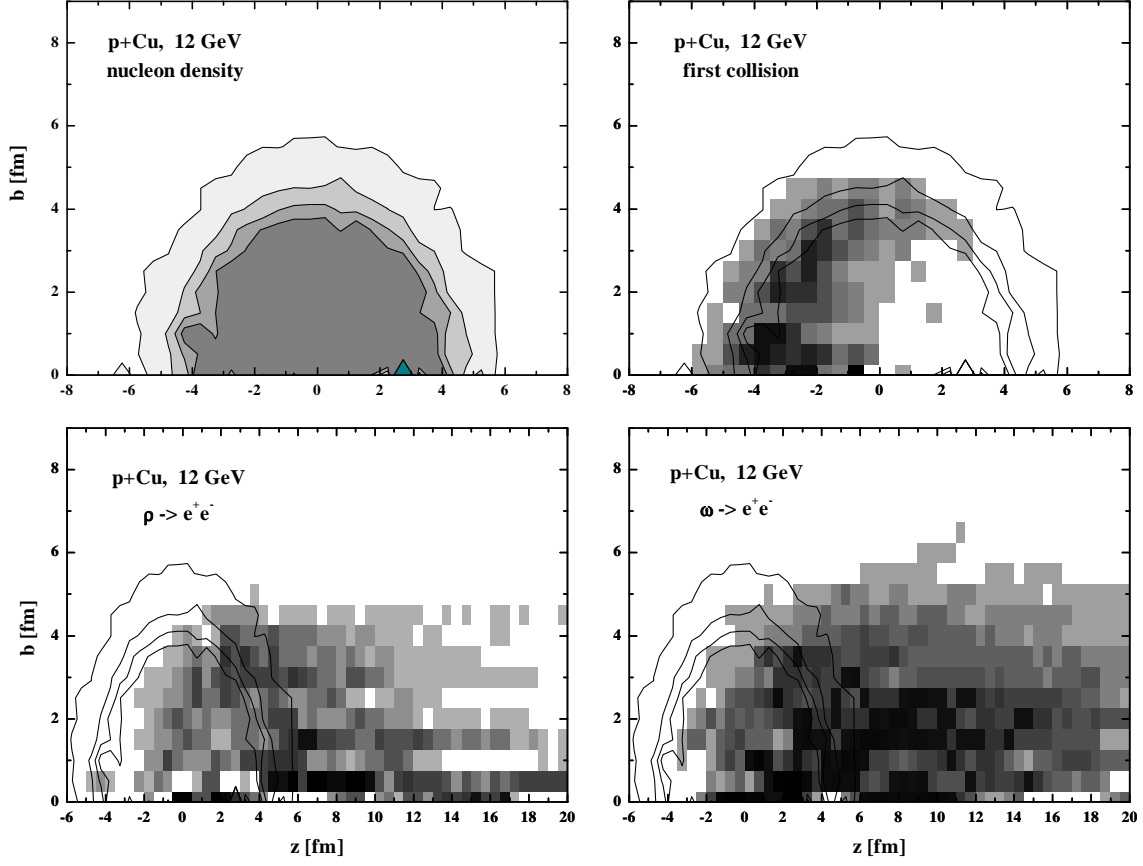


Figure 4: Upper left part: the average density distribution of a Cu -nucleus at rest in the laboratory; upper right part: the spatial distribution in the first pN collisions; lower parts: the spatial distribution for ρ -meson (left) and ω -meson (right) decays to dileptons. The contour lines correspond to nucleon densities of $0.1\rho_0$, $0.4\rho_0$, $0.6\rho_0$ and $0.8\rho_0$, respectively, and the dark shaded area to $\rho \geq 0.8\rho_0$.

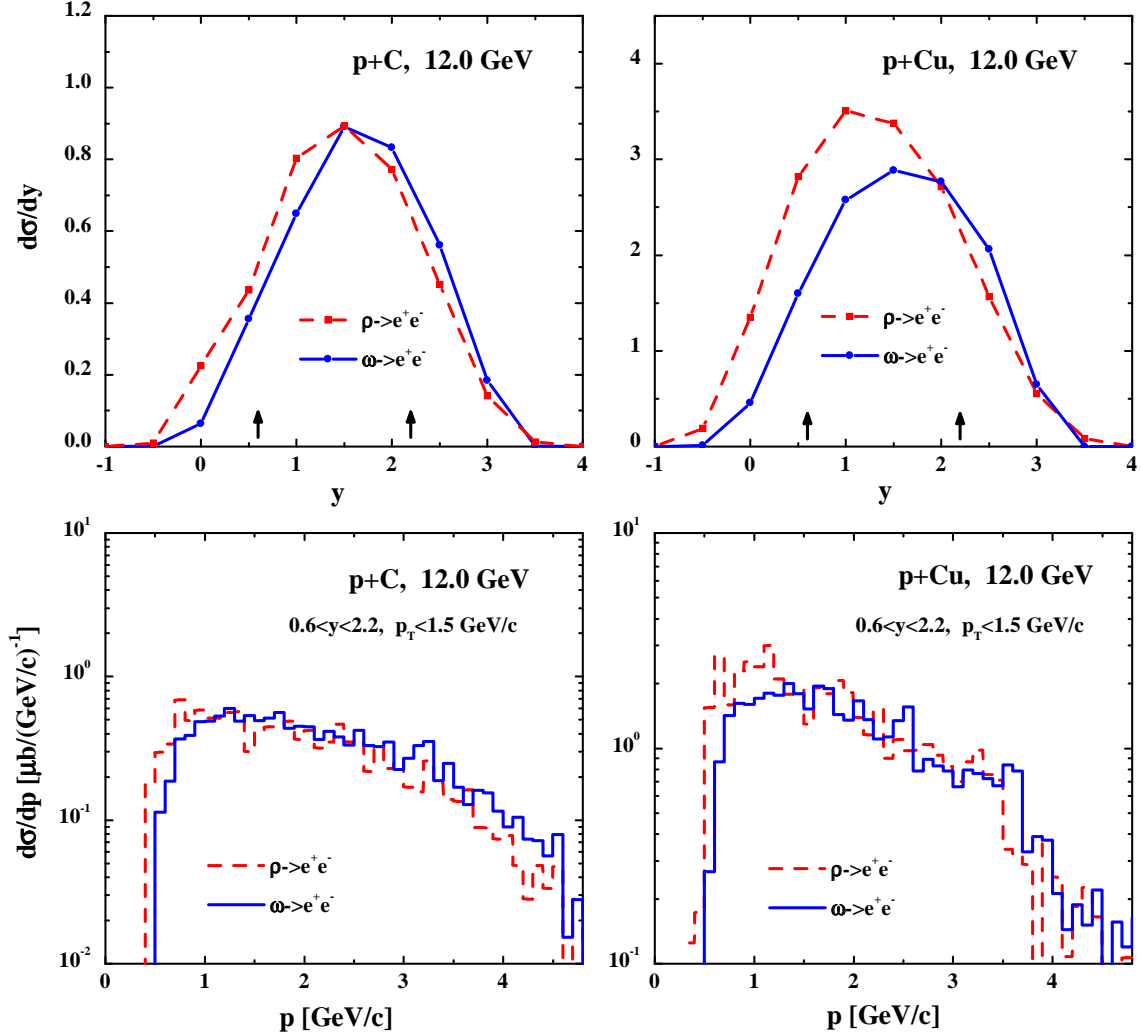


Figure 5: Upper part: the laboratory rapidity distributions $d\sigma/dy$ for $\rho \rightarrow e^+e^-$ (dashed lines) and $\omega \rightarrow e^+e^-$ (solid lines) for $p+C$ (left) and $p+Cu$ (right) at 12 GeV. The arrows indicate the experimental rapidity window ($0.6 \leq y \leq 2.2$). Lower part: the momentum distribution $d\sigma/dp$ for $\rho \rightarrow e^+e^-$ (dashed lines) and $\omega \rightarrow e^+e^-$ (solid lines) for $p+C$ (left) and $p+Cu$ systems (right) at 12 GeV calculated with experimental cuts in rapidity ($0.6 \leq y \leq 2.2$) and p_T ($p_T < 1.5$ GeV/c).